

Charge-state changes of substitutional nitrogen impurities in silicon induced by additional impurities and defects

Hisayoshi Itoh, Kouichi Murakami, Kōki Takita, and Kohzoh Masuda
Institute of Materials Science, University of Tsukuba, Sakura, Ibaraki 305, Japan

(Received 19 June 1986; accepted for publication 13 January 1987)

Charge states of substitutional N impurities (N_s) in Si are found to be controllable by doping with P, B, and O impurities in N-ion implanted and subsequently pulsed-laser annealed Si (Si:N system). Electron-spin resonance measurements of the Si:N system doped with P, B, or O impurities show that the spin density of neutral N_s (N_s^0) decreases because of doping with these impurities. Compensation by multiple doping with equal amounts of P and B impurities leaves the density of N_s^0 essentially unchanged. These results yield evidence for charge-state changes of N_s due to the Fermi level shift. Oxygen doping is found to introduce donors. Three charge states, i.e., positive (N_s^+), neutral (N_s^0), and negative (N_s^-) are assigned to off-center substitutional N in Si.

I. INTRODUCTION

Nitrogen (N) impurities doped in Si are known to pin dislocations^{1,2} in Si and suppress thermal oxidation^{3,4} of Si. It was reported that N impurities retard silicide formation.⁵ In addition, buried silicon-nitride layer formed by N-ion implantation is useful for an insulator and a diffusion barrier for impurities.^{4,6,7} Therefore, N impurities in Si have been of technological interest in recent years.

There is, however, little information about substitutional or off-center substitutional N impurities (N_s) in Si, in contrast to the other group-V elements. This is attributed to the difficulty of introducing N_s into Si by the conventional doping techniques.⁸ In fact, the equilibrium solid solubility of N in Si is low ($4.5 \pm 1.0 \times 10^{15}$ atoms/cm³) (Ref. 9) as compared with that of the other donor- and acceptor-type impurities. On the other hand, it is known that N impurities are introduced into off-center substitutional sites of Si in excess of their solid solubility by means of N-ion implantation and subsequent pulsed-laser annealing (PLA).^{10,11} This stimulated many kinds of experiments for N impurities in Si; e.g., deep-level transient spectroscopy (DLTS),^{12,13} photoluminescence,¹⁴⁻¹⁶ infrared absorption,^{17,18} and electron spin resonance (ESR).^{15,19-21} This also stimulated theoretical studies²²⁻²⁴ of substitutional N impurities in Si. The electronic levels of N_s , however, have not as yet been clarified. Determination of the charge states of N_s is needed to understand electrical characteristics and diffusion kinetics for N in Si. This can be accomplished by the introduction of donor-type¹⁹ or acceptor-type impurities into Si with N_s (Si:N system).

Moreover, the interactions between N and O impurities have been a growing interest. It was reported that N impurities enhance oxygen precipitation in Czochralski (CZ) Si wafers.²⁵ Stein²⁶ reported interactions of N pairs with O in pulsed-laser annealed Si and suggested that the interaction is controlled by O, which diffuses to sites near Si-N pairs. We found that O impurities have an effect on thermal annealing behavior of N_s .²¹

In this paper we report the effects of introducing P, B, and O impurities into the Si:N system and then discuss the

charge states and electronic levels of N_s in Si. The impurity doping effects are investigated by the ESR measurements of various Si:N samples with additionally implanted impurities.

II. EXPERIMENTAL PROCEDURE

N ions (N_2^+) were implanted in CZ, B-doped (100) Si wafers with the resistivity of 30~50 Ω cm at an acceleration energy of 70 keV. P ions (P^+), B ions (B^+), and O ions (O_2^+) were subsequently implanted at acceleration energies of 70, 30, and 80 keV, respectively, to approximately overlap the profiles for N. The mean projected ranges (R_p) for 70 keV N_2^+ , 70 keV P^+ , 30 keV B^+ , and 80 keV O_2^+ are about 940, 850, 970, and 940 \AA , respectively.²⁷ The standard deviations for N_2 , P, B, and O_2 ions are about 400, 340, 370, and 390 \AA , respectively.²⁷ The ion implantation dose varied from 10^{12} to 10^{15} /cm² for P and B ion implantations and from 10^{12} to 10^{16} /cm² for O ion implantation. All the ion implantations were made at room temperature (RT) and in a vacuum lower than 4×10^{-6} Torr. The dose rates of the ion-implanted impurities were lower than 0.5 $\mu\text{A}/\text{cm}^2$.

All the ion implanted samples were annealed with a Q-switched ruby laser ($\lambda = 694$ nm, pulse duration = 40 ns) at energy densities from 1.2 to 1.5 J/cm². The anneal-beam irradiated samples in air through a quartz tube to homogenize a spatial variation in the beam intensity.

ESR measurements of these samples were made with a X-band (9-GHz) microwave incident upon TE_{011} cylindrical cavity at RT. For the measurement of conduction and/or donor electrons in P-doped Si:N samples, the ESR measurements were made at about 77 K. To avoid the saturation of ESR absorption of neutral N_s (N_s^0), the microwave power was made lower to 2 mW. The absolute number of N_s^0 in Si was determined relative to the known number of Mn^{2+} in MgO, as a spin standard. Thus, a variation in cavity Q does not affect our evaluation of the spin density of N_s^0 . The absolute spin density was estimated to be uncertain by a factor less than 3, but the uncertainty in the relative density was less than $\pm 15\%$.

III. RESULTS AND DISCUSSION

A. Phosphorus and boron doping

Figure 1 shows ESR spectra of Si:N, P-doped Si:N (Si:N:P) and B-doped Si:N (Si:N:B) samples observed at RT. Three hyperfine (hf) lines of N_s^0 are clearly observed in the Si:N sample with $2 \times 10^{14} N_2^+ / \text{cm}^2$, as shown in Fig. 1(a). It was reported by Brower¹⁰ that the SL5 center assigned to N_s^0 has C_{3v} symmetry about $\langle 111 \rangle$ at temperatures below 100 K. This indicates that N is in off-center substitutional site rather than substitutional site of Si. Furthermore, we found from ESR measurements at RT that N_s^0 is isotropic (T_d symmetry) because of a motional effect.¹¹ In this case the g value and hf constant A are 2.0065 ± 0.0005 and 16.0 ± 0.3 G, respectively. It is found from Fig. 1 that these isotropic values are not changed by doping with P or B in the Si:N sample, but intensities for the hf lines of N_s^0 are decreased by P or B doping, as shown in Figs. 1(b) and 1(c). Possible effects of strong spin-spin interactions between localized spin of N_s^0 and degenerate P donor electrons must be considered when we interpret a decrease in N_s^0 . However, since no significant change in ESR linewidth and g factor of N_s^0 was observed in the Si:N:P system, the decrease in N_s^0 cannot be explained by spin-spin interactions between N_s^0 and P donor electrons. The same result was obtained in dangling bonds of Si in degenerate Si:P systems.²⁸

Figure 2 shows the effects of various doses of P and B impurities on N_s^0 in the Si:N samples with $2 \times 10^{14} N_2^+ / \text{cm}^2$ and $5 \times 10^{13} N_2^+ / \text{cm}^2$. The Ar impurity effect is also shown in Fig. 2 for comparison. Here, an acceleration energy of Ar ions (Ar^+) was 80 keV and R_p is about 770 Å. The spin density of N_s^0 decreases dramatically with P or B doses above certain critical doses. The critical doses of P and B for the Si:N sample with $2 \times 10^{14} N_2^+ / \text{cm}^2$ are approximately $4 \times 10^{13} \text{P}^+ / \text{cm}^2$ and $2 \times 10^{13} \text{B}^+ / \text{cm}^2$, respectively. Aver-

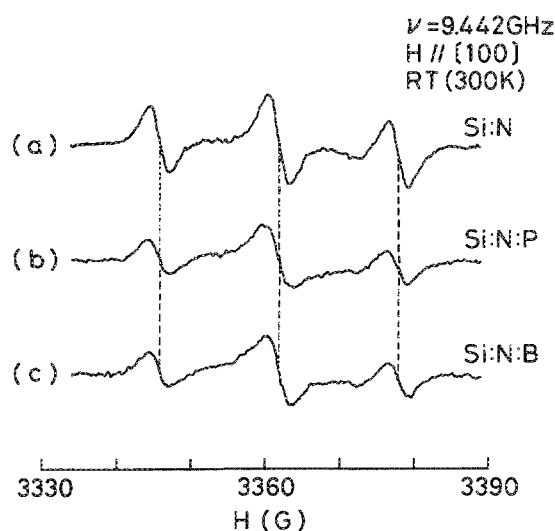


FIG. 1. (a) ESR spectrum of N_s^0 observed in the Si:N sample with a dose of $2 \times 10^{14} N_2^+ / \text{cm}^2$. Doping effects of P and B on the N_s^0 -ESR spectrum are shown in (b) and (c), respectively. Doses of P and B are $1 \times 10^{14} \text{P}^+ / \text{cm}^2$ and $5 \times 10^{13} \text{B}^+ / \text{cm}^2$, respectively. These spectra were observed at room temperature for $H \parallel [100]$.

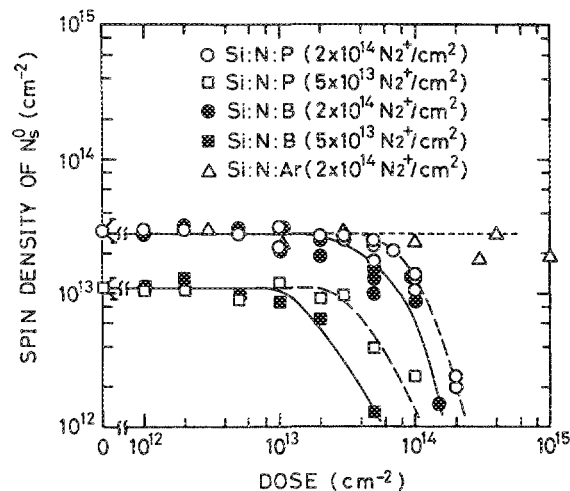


FIG. 2. P-, B-, and Ar-doping effects upon the neutral substitutional N impurity (N_s^0) density in the Si:N samples with N doses of $2 \times 10^{14} N_2^+ / \text{cm}^2$ and $5 \times 10^{13} N_2^+ / \text{cm}^2$. The abscissa indicates 70-keV- P^+ , 30-keV- B^+ , and 80-keV- Ar^+ dose levels.

age concentrations (dose/ $2R_p$) of P and B for these critical doses are about $2 \times 10^{18} / \text{cm}^3$ and $1 \times 10^{18} / \text{cm}^3$, respectively. For the Si:N sample with $5 \times 10^{13} N_2^+ / \text{cm}^2$, the critical doses of P and B are about $2 \times 10^{13} \text{P}^+ / \text{cm}^2$ and $1 \times 10^{13} \text{B}^+ / \text{cm}^2$, respectively. In contrast to P and B doping, N_s^0 remains constant for Ar doping to a dose of about $1 \times 10^{15} \text{Ar}^+ / \text{cm}^2$. Results of Hall effect and Rutherford backscattering measurements²⁹ show that 100% of the P and B impurities (up to concentrations of $\sim 5 \times 10^{21} / \text{cm}^3$ and $\sim 1 \times 10^{21} / \text{cm}^3$, respectively) are electrically activated by PLA. It was also reported²⁹ that no macroscopic defects exist after PLA in Si doped with P and B up to these concentrations. In the present study the maximum concentration of P and B, corresponding to a dose of $1 \times 10^{15} / \text{cm}^2$, is about $1 \times 10^{20} / \text{cm}^3$. Consequently, ion-implanted P and B impurities are completely activated and the crystallinity of the Si:N system is not affected significantly by these P- or B-doping levels.

The critical P dose necessary to decrease N_s^0 is found to be dependent upon the implanted N dose rather than the spin density. This was determined from measurements on a Si:N sample that had been implanted with $2 \times 10^{15} N_2^+ / \text{cm}^2$. The spin density of N_s^0 for this higher dose was essentially the same as that for $2 \times 10^{14} N_2^+ / \text{cm}^2$, but the critical P dose was about $7 \times 10^{13} \text{P}^+ / \text{cm}^2$ compared to $4 \times 10^{13} \text{P}^+ / \text{cm}^2$. Thus, the decrease in N_s^0 is caused by P doping rather than by direct interaction between N and P in Si.

The P-doping effect on the spin density of N_s^0 can be interpreted by change in charge states of N_s . In this case a negative charge state of N_s (N_s^-) is probably formed in the Si:N:P system. It was reported experimentally that N_s^0 is a deep-level donor and N-related paramagnetic defects exist in pulsed-laser annealed Si:N system.^{10,11} Electronic levels for N_s^0 , N_s^- , and other N-related (ΣN) defects are schematically illustrated in Fig. 3.¹⁹ Without P doping, the Fermi level (E_F) is thought to be located between a level of N_s^0 and that

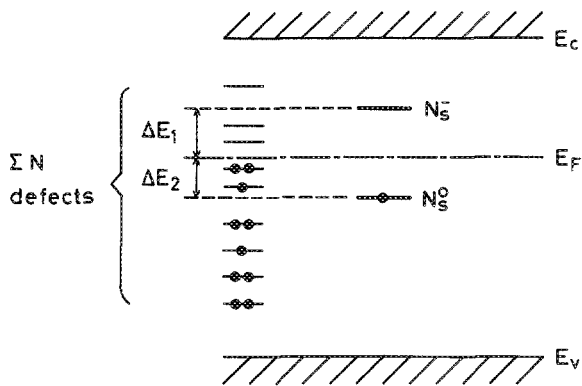


FIG. 3. Schematic energy diagram for N_s^- , N_s^0 , and other ΣN defects in Si:N. Levels with one or two electrons are in singly occupied or doubly occupied states, respectively.

of N_s^- . Doping with P donors will cause E_F to rise because P-donor electrons are trapped by levels of other ΣN defects, levels between the initial E_F and the level of N_s^- (ΔE_1 in Fig. 3). In the P-dose range below the critical dose, P-donor electrons are trapped only by levels of ΣN defects in ΔE_1 and the density of N_s^0 does not change. Above the critical P dose, E_F is shifted towards the level of the P, and so P donor electrons are trapped by N_s^0 to form diamagnetic N_s^- states in the Si:N:P system.¹⁹

To examine conduction and/or donor (C/D) electrons trapped by ΣN defects and N_s^0 , ESR measurements of the Si:N:P samples were performed at about 77 K. ESR spectra observed are shown in Fig. 4. The spectrum of C/D electrons

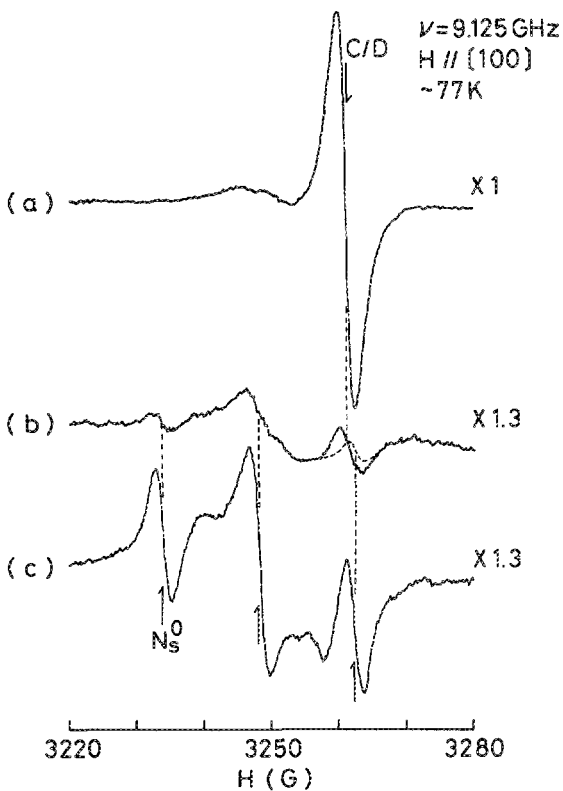


FIG. 4. ESR spectra of the Si:N:P samples with $1 \times 10^{14} P^+$ /cm² observed at about 77 K for $H \parallel [100]$. N doses are (a) $5 \times 10^{13} N_2^+$ /cm², (b) $2 \times 10^{14} N_2^+$ /cm², and (c) $1 \times 10^{15} N_2^+$ /cm². Both conduction and/or donor (C/D) electrons and N_s^0 are observed in (b).

($g = 1.999$) is observed in the Si:N:P sample with $5 \times 10^{13} N_2^+$ /cm² and $1 \times 10^{14} P^+$ /cm² as shown in Fig. 4(a). It is found from Figs. 4(b) and 4(c) that C/D electrons decrease with increasing N dose. In the Si:N:P with $1 \times 10^{15} N_2^+$ /cm² and $1 \times 10^{14} P^+$ /cm², C/D electrons cannot be seen, while N_s^0 can be observed. Figure 5 shows N dose dependence of the spin density of C/D electrons and N_s^0 in the Si:N:P samples with $1 \times 10^{14} P^+$ /cm² and $5 \times 10^{13} P^+$ /cm². N dose dependence¹¹ of N_s^0 in the Si:N system is also represented by a dashed line in Fig. 5. The decrease in C/D electrons by doping with N indicates that ΣN defects with deep levels increase with N dose, and they trap C/D electrons. It should be also stressed that the number of the trap centers is approximately 50%–100% of that of the implanted N_2^+ . This suggests that N pairs observed by Stein¹⁷ in Si implanted with N may be dominant in ΣN . For N_2 dose $> 10^{14}$ /cm², N_s^0 becomes observable, while the C/D electrons almost disappear. The difference between the spin density of N_s^0 in the Si:N system and that in the Si:N:P system probably corresponds to a density of N_s^- in the Si:N:P system.

Similarly to the P doping, B doping decreases N_s^0 in the Si:N system, as shown in Fig. 2. This can also be explained by change in the charge states of N_s^- . In this case no shallow donors are added so that doping with B in the Si:N system causes E_F to fall. If the initial E_F is located just below the level of N_s^- within an energy difference of 0.06 eV, an increase in the spin density of N_s^0 should be observed at 300 K initially for B doping. However, the density of N_s^0 is not influenced within the experimental accuracy (15%) by the doping with B in the dose range below critical doses of about 10^{13} /cm². This suggests that the initial E_F is not located just below the level of N_s^- but near the middle of the levels of N_s^0 and N_s^- . Thus, below the critical dose, B acceptors capture electrons from ΣN defects whose levels are located between the initial E_F and the level of N_s^0 (ΔE_2 in Fig. 3). In the B-dose range above the critical dose, E_F is shifted towards the

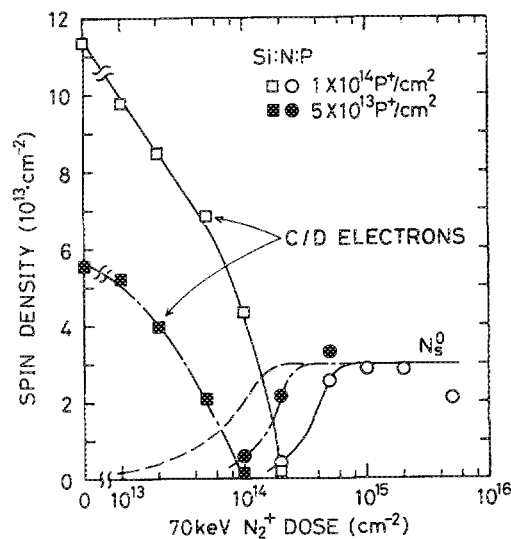


FIG. 5. Conduction and/or donor (C/D) electrons (squares) and N_s^0 (circles) in the Si:N:P samples with $1 \times 10^{14} P^+$ /cm² (open) and $5 \times 10^{13} P^+$ /cm² (closed), as functions of N_2^+ dose. N dose dependence of N_s^0 without P doping is shown by dashed line.

acceptor level of B, and then N_s with a positive charge (N_s^+) is possibly formed, which cannot be detected by ESR measurements. In contrast to this idea, one may consider that the decrease in N_s^0 by the B doping is due to pair formation of N_s and substitutional B impurities, and such a pair has no unpaired electron. This latter possibility must be ruled out because of the results of multiple doping with P and B in the Si:N system, as described later.

To confirm the idea of charge-state changes, multiple doping with P and B was carried out in the Si:N system. In this approach doping effects are independent of ΣN defects since electronic levels for B acceptors and P donors are most shallow. Figure 6 shows the results of multiple doping with P and B impurities in the Si:N system. The spin density of N_s^0 in the Si:N sample with $2 \times 10^{14} N_2^+ / \text{cm}^2$ is about $3.8 \times 10^{13} / \text{cm}^2$ and decreases down to $1.9 \times 10^{13} / \text{cm}^2$ and $1 \times 10^{12} / \text{cm}^2$ with B doping at doses of $5 \times 10^{13} B^+ / \text{cm}^2$ and $1.5 \times 10^{14} B^+ / \text{cm}^2$, respectively (see Figs. 2 and 6). In the Si:N:B with $5 \times 10^{13} B^+ / \text{cm}^2$, N_s^0 increases substantially when the P doping is around a dose of $5 \times 10^{13} P^+ / \text{cm}^2$. A similar result is obtained for P doping in the Si:N:B with $1.5 \times 10^{14} B^+ / \text{cm}^2$. These results illustrate the compensating effect between P donors and B acceptors and show that the decrease in N_s^0 by B or P doping is not caused by N_s -P or N_s -B pairing. We conclude, therefore, that the variation in N_s^0 observed in the Si:N:B and Si:N:P systems is due to changes in the charge states of the N_s .

B. Oxygen doping

The effect of doping with O impurities on N_s^0 in the Si:N system was examined to investigate interactions between N and O impurities (or O-related defect centers). Figure 7 shows the O-doping effect on N_s^0 for the Si:N samples with $2 \times 10^{14} N_2^+ / \text{cm}^2$ and $5 \times 10^{13} N_2^+ / \text{cm}^2$. The Ar-doping effect is also shown for comparison. For the Si:N:O sample, the spin density of N_s^0 changes anomalously in O dose range between $1 \times 10^{14} O_2^+ / \text{cm}^2$ and $1 \times 10^{15} O_2^+ / \text{cm}^2$, i.e., N_s^0 decreases with increasing O dose in the dose range from

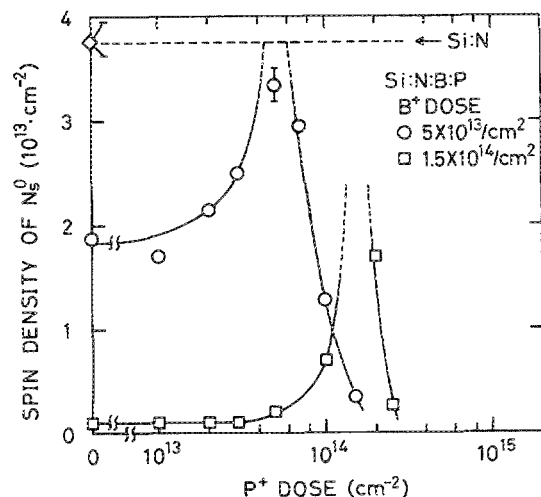


FIG. 6. P-doping effect on N_s^0 in the Si:N:B samples with $5 \times 10^{13} B^+ / \text{cm}^2$ and $1.5 \times 10^{14} B^+ / \text{cm}^2$. N dose in both samples is $2 \times 10^{14} N_2^+ / \text{cm}^2$. Broken line indicates the spin density of N_s^0 in the Si:N with $2 \times 10^{14} N_2^+ / \text{cm}^2$.

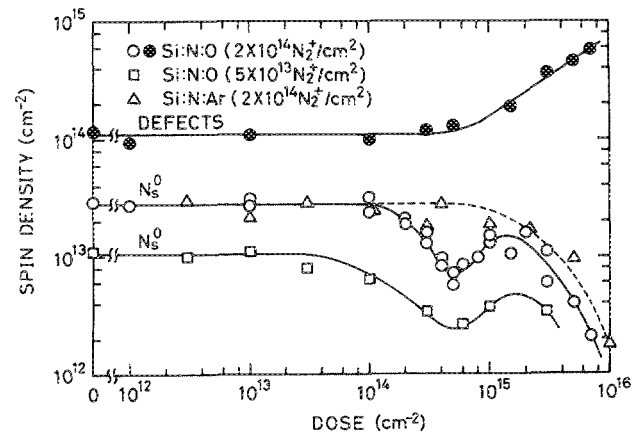


FIG. 7. O- and Ar-doping effects upon N_s^0 density in the Si:N samples with $2 \times 10^{14} N_2^+ / \text{cm}^2$ and $5 \times 10^{13} N_2^+ / \text{cm}^2$. The abscissa indicates 80-keV- O^{2+} and 80-keV- Ar^+ dose levels. The spin density of residual paramagnetic defects is also shown for the Si:N:O sample with $2 \times 10^{14} N_2^+ / \text{cm}^2$ after pulsed-laser annealing.

1×10^{14} to $5 \times 10^{14} O_2^+ / \text{cm}^2$ and increases in the range from 5×10^{14} to $1 \times 10^{15} O_2^+ / \text{cm}^2$. No significant change in N_s^0 is seen below $1 \times 10^{14} O_2^+ / \text{cm}^2$. In the dose range above $1 \times 10^{15} O_2^+ / \text{cm}^2$, N_s^0 decreases with increasing O dose because of imperfect recrystallization like Ar implantation³⁰ above $1 \times 10^{15} Ar^+ / \text{cm}^2$. The anomalous change in N_s^0 is not observed in Ar doping.

He-ion implantation and multiple doping with O and B (or P) were performed to investigate the anomalous change in N_s^0 in the Si:N:O system. The results of He⁺ implantation are shown in Fig. 8 for the Si:N:O sample with $2 \times 10^{14} N_2^+ / \text{cm}^2$ and $5 \times 10^{14} O_2^+ / \text{cm}^2$ in which the largest anomalous decrease is observed. N_s^0 in the Si:N:O system is increased by defect production with He-ion implantation, such as the case of the Si:N:P system. This suggests that new donor levels related with O impurities are formed in the Si:N:O system, and N_s^- states are generated.

Figure 9 shows B- and P-doping effects on N_s^0 for the Si:N:O samples with $3 \times 10^{14} O_2^+ / \text{cm}^2$ and 5×10^{14}

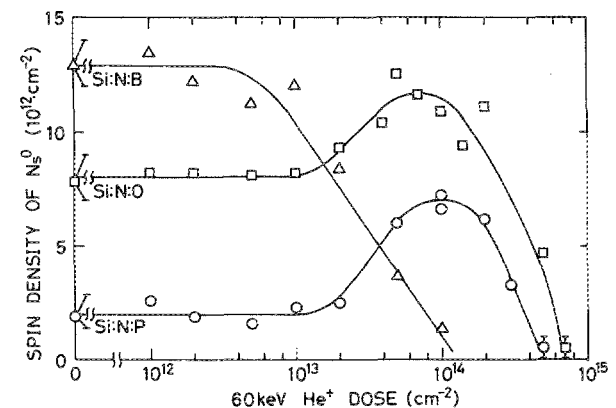


FIG. 8. He-ion implantation effect on N_s^0 in the Si:N:P sample with $2 \times 10^{14} P^+ / \text{cm}^2$, the Si:N:B sample with $1 \times 10^{14} B^+ / \text{cm}^2$ and the Si:N:O sample with $5 \times 10^{14} O_2^+ / \text{cm}^2$. N dose in all samples is $2 \times 10^{14} N_2^+ / \text{cm}^2$. The projected range of 60 keV He⁺ is about $0.8 \mu\text{m}$.

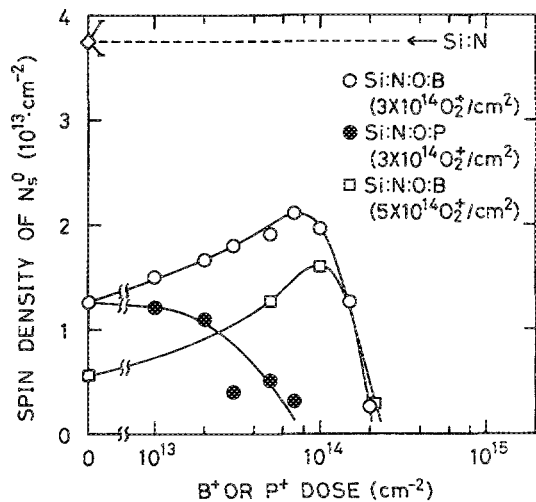


FIG. 9. B- and P-doping effects on N_s^0 in the Si:N:O samples with 3×10^{14} O_2^+ /cm² and 5×10^{14} O_2^+ /cm². N dose in both samples is 2×10^{14} N_2^+ /cm². Broken line represents the initial density of N_s^0 in the Si:N.

O_2^+ /cm². The spin density of N_s^0 in the Si:N:O system increases by B doping in the dose range up to 1.5×10^{14} B^+ /cm². On the other hand, N_s^0 decreases by P doping. The quantitative change in N_s^0 due to B or P doping in the Si:N:O system suggests strongly that new O-related donors are formed and then N_s^0 changes to N_s^- by O doping in the Si:N. It leads to decrease in N_s^0 . In regard to O-related donors, it was recently reported that a donor in CZ Si formed by PLA may be related with O impurities.³¹ It is well known that thermal donors originate from O impurities.³²

The increase in N_s^0 with O dose in the dose range from 5×10^{14} to 1×10^{15} O_2^+ /cm² can be explained by significant production of other defects with levels deeper than that of N_s^- . Introduction of a high concentration of O impurities causes production of deep-level defects in Si. In fact, residual paramagnetic defects increase in O dose range above 5×10^{14} O_2^+ /cm², as shown in Fig. 7. These defects trap an electron from N_s^- formed in the Si:N:O system and then N_s^- changes to N_s^0 .

It is also found from Fig. 9 that N_s^0 in the Si:N:O samples with 3×10^{14} O_2^+ /cm² and 5×10^{14} O_2^+ /cm² recovers by B doping to about 60% and 40% of that in the Si:N sample, respectively. The anomalous decrease in N_s^0 is partly due to change in the charge states of N_s . The other part of decrement in N_s^0 is possibly caused by interactions between N_s and O impurities such as pairing of these impurities. In addition, the donor levels related with O impurities are thought to be formed most efficiently at a dose of 5×10^{14} O_2^+ /cm² (see Fig. 7). The decrements of N_s^0 by O doping at 5×10^{14} O_2^+ /cm² were 2×10^{13} /cm² and 8×10^{12} /cm² for the Si:N samples with 2×10^{14} N_2^+ /cm² and 5×10^{13} N_2^+ /cm², respectively. The decrement depends on N concentration in the Si:N:O system. This result suggests that a part of the decrement in N_s^0 is due to interactions between N_s and O.

C. Electronic energy levels

It is difficult to determine exactly the electronic levels for N_s in Si from the concentrations of P or B impurities in

the Si:N system because some kinds of defects such as ΣN exist in the Si:N system. Approximate levels for N_s are estimated from the results of N dose dependence of C/D electrons and N_s^0 in the Si:N:P system and from DLTS measurements for the Si:N system. It should be stressed that, for example, ESR signals of both C/D electrons and N_s^0 can be observed in the Si:N:P sample with 2×10^{14} N_2^+ /cm² and 1×10^{14} P^+ /cm², as shown in Figs. 4(b) and 5. The spin density of P donor electrons and N_s^0 becomes about 2% of that in the Si:P sample only with 1×10^{14} P^+ /cm² and about 10% of that in the Si:N sample only with 2×10^{14} N_2^+ /cm², respectively. The latter shows that about 90% of N_s is in the state of N_s^- . These indicate that electrons occupy about 2% of P donor level and about 90% of N_s^- level at 77 K. Taking account of the Fermi-Dirac distribution function at 77 K, a difference in the energy levels between P donor and N_s^- is estimated to be about 40 meV. Since the maximum concentration of P is about 1×10^{19} /cm³ in the Si:N:P sample with 1×10^{14} P^+ /cm², the P donors form an impurity band in Si. However, it was assumed here that the width of the impurity band is narrow. Thus, the level of N_s^- is estimated to be about 80 meV under the bottom of the conduction band of Si ($E_c - 0.08$ eV). Pantelides and Sah³³ reported that a calculated level of N_s^- is $E_c - 52.5$ meV. Our estimated value is in reasonable agreement with the calculated value. To investigate deep levels in pulsed-laser annealed Si:N system, DLTS measurements of the Si:N system were performed. Three deep levels of $E_c - 0.31$ eV, $E_c - 0.42$ eV, and $E_c - 0.56$ eV were observed. In particular, the level of $E_c - 0.31$ eV increased with N dose in the Si:N system. It seems that the level of $E_c - 0.31$ eV compares with a value ($E_c - 335.9$ meV) for N_s^0 calculated by Pantelides and Sah.³³ More work is needed, however, for assignment of these observed levels. The DLTS and barrier-controlled ESR measurements are now in progress for the Si:N system to determine exact levels of N_s^- and N_s^0 .

He-ion implantation of the Si:N:P and Si:N:B systems was performed to further check the approximate levels of N_s^0 and N_s^- . These are schematically illustrated in Fig. 10(a). Figure 8 shows the result of 60-keV-He⁺ implantation in the Si:N:P with 2×10^{14} N_2^+ /cm² and 2×10^{14} P^+ /cm² and in the Si:N:B with 2×10^{14} N_2^+ /cm² and 1×10^{14} B^+ /cm². The initial spin densities of N_s^0 in the Si:N:P and Si:N:B samples decrease from 3.0×10^{13} /cm² to 2.0×10^{12} /cm² and 1.3×10^{13} /cm², respectively, because of the charge-state changes of N_s^0 , as shown in Figs. 10(b) and 10(c) (see Sec. A). The He-ion implanted samples were not annealed in this case. The increase in N_s^0 in the Si:N:P sample is clearly observed with He-ion dose from 2×10^{13} He⁺/cm² to 3×10^{14} He⁺/cm², but is not observed in the Si:N:B sample. Our interpretation for the He⁺ implantation effect is illustrated in Figs. 10(d) and 10(e) for the Si:N:P and Si:N:B systems, respectively. It was reported that He-ion implantation induces several deep-level defects (electron traps and hole traps) such as O-vacancy pairs and divacancy centers in Si,³⁴ similarly in the case for electron irradiation. Since the levels of induced defects are thought to be distributed in Si band gap, these levels cause gradually E_F to shift towards the middle of the band gap with increasing the He dose. Therefore,

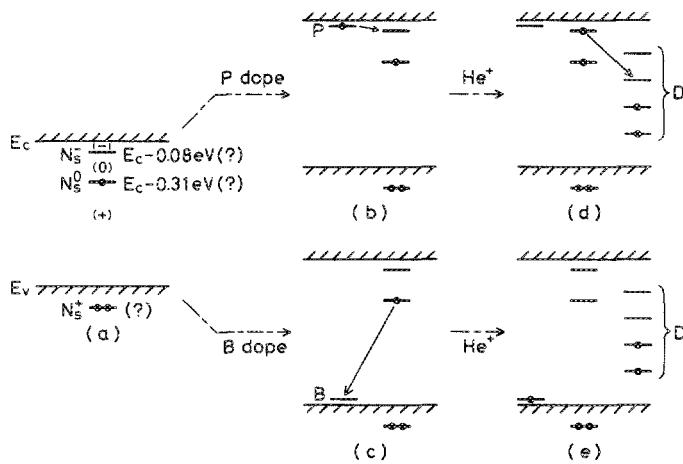


FIG. 10. (a) Schematic energy diagram of the substitutional N (N_s) in Si. Signs of +, 0, and - indicate charge states of N_s . A level of N_s^+ indicating a bonding state of Si-N is assumed to be under the top of the valence band. P- and B-doping effects on N_s are shown in (b) and (c), respectively. He⁺ implantation effect is schematically illustrated in (d) and (e) for Si:N:P and Si:N:B systems, respectively. D represents levels of defects induced by He⁺ implantation. Solid arrows represent an electron trapping.

the results of He-ion implantation can be interpreted by the Fermi level shift if the electronic levels of N_s (N_s^0 and N_s^-) are located in the upper side of Si band gap.

IV. CONCLUSIONS

We have investigated the effects of doping with P (donor-type) and B (acceptor-type) impurities on substitutional N impurities (N_s) in the Si:N system in order to clarify electronic states of N_s in Si. The spin density of neutral substitutional N impurities (N_s^0) in the Si:N system decreases by introduction of P or B impurities. He-ion implantation causes increase in N_s^0 for Si:N:P system, while it causes decrease in N_s^0 for Si:N:B system. Multiple doping with equal amounts of P and B impurities shows no significant change in N_s^0 , indicating their compensating effects. From these results, we conclude that substitutional N impurities (N_s) in Si exhibit at least three controllable charge states, i.e., neutral (N_s^0), negative (N_s^-), and positive (N_s^+) states. N_s^- and N_s^+ states are formed in the Si:N:P and Si:N:B systems, respectively, depending on the Fermi level position.

Furthermore, the effects of doping with O impurities on N_s^0 are first investigated. The spin density of N_s^0 decreases anomalously by O doping in the dose range between 1×10^{14} O₂⁺/cm² and 1×10^{15} O₂⁺/cm². Both He-ion implantation and B doping in the Si:N:O system cause increase in N_s^0 , whereas P doping causes its decrease. The results yield evidence that new O-related donors are generated by pulsed-laser annealing, and then N_s^- states are formed in the Si:N:O system.

ACKNOWLEDGMENTS

The authors would like to thank O. Eryu and T. Masaki for their assistance in the experiments and Professor H. Sue-

matsu for his support in the ESR experiments. We would like to express our appreciation to Dr. Y. Yuba for DLTS measurements and valuable discussions. This work was partly supported by a Grant-in Aid for the Special Project Research (1985-1987) on Ion Beam Interactions with Solids from the Ministry of Education, Science and Culture.

¹T. Abe, K. Kikuchi, S. Shirai, and S. Muraoka, in *Semiconductor Silicon 1981*, edited by H. R. Huff, R. J. Kriegler, and Y. Takeishi (Electrochemical Society, Pennington, NJ, 1981), p. 54.

²K. Sumino, I. Yonenaga, M. Imai, and T. Abe, *J. Appl. Phys.* **54**, 5016 (1983).

³W. J. M. J. Josquin and Y. Tamminga, *J. Electrochem. Soc.* **129**, 1803 (1982).

⁴W. J. M. J. Josquin, *Nucl. Instrum. Methods* **209/210**, 581 (1983).

⁵K. T. Ho, C.-D. Lien, and M.-A. Nicolet, *J. Appl. Phys.* **57**, 232 (1985).

⁶R. J. Dexter, S. B. Watelski, and S. T. Picraux, *Appl. Phys. Lett.* **23**, 455 (1973).

⁷P. L. F. Hemment, R. F. Peart, M. F. Yao, K. G. Stephens, R. J. Chater, J. A. Kilner, D. Meekison, G. R. Booker, and R. P. Arrowsmith, *Appl. Phys. Lett.* **46**, 952 (1985).

⁸P. V. Pavlov, E. I. Zorin, D. I. Tetelbaum, and A. F. Khokhlov, *Phys. Status Solidi A* **35**, 11 (1976).

⁹Y. Yatsurugi, N. Akiyama, Y. Endo, and T. Nozaki, *J. Electrochem. Soc.* **120**, 975 (1973).

¹⁰K. L. Brower, *Phys. Rev. B* **26**, 6040 (1982).

¹¹K. Murakami, K. Masuda, Y. Aoyagi, and S. Namba, *Physica* **116B**, 564 (1983).

¹²Y. Tokumaru, H. Okushi, T. Masui, and T. Abe, *Jpn. J. Appl. Phys.* **21**, L443 (1982).

¹³K. Nauka, M. S. Goorsky, H. C. Gatos, and J. Lagowski, *Appl. Phys. Lett.* **47**, 1341 (1985).

¹⁴H. C. Alt and L. Tapfer, in *Proceedings of the 13th International Conference on Defects in Semiconductors*, edited by L. C. Kimerling and J. M. Parsey, Jr. (The Metallurgical Society of American Institute of Mining, Metallurgical and Petroleum Engineers, Warrendale, PA, 1985), p. 833.

¹⁵K. Murakami, H. Itoh, K. Takita, K. Masuda, and T. Nishino, in *Proceedings of the 17th International Conference on Physics of Semiconductors*, edited by J. D. Chadi and W. A. Harrison (Springer, New York, 1985), p. 1493.

¹⁶A. Dörnen, G. Pensl, and R. Sauer, *Phys. Rev. B* **33**, 1495 (1986).

¹⁷H. J. Stein, in *Proceedings of the 13th International Conference on Defects in Semiconductors*, edited by L. C. Kimerling and J. M. Parsey, Jr. (The Metallurgical Society of American Institute of Mining, Metallurgical and Petroleum Engineers, Warrendale, PA, 1985), p. 839.

¹⁸H. J. Stein, *Appl. Phys. Lett.* **47**, 1339 (1985).

¹⁹K. Murakami, H. Itoh, K. Takita, and K. Masuda, *Appl. Phys. Lett.* **45**, 176 (1984).

²⁰M. Sprenger, E. G. Sieverts, S. H. Muller, and C. A. J. Ammerlaan, *Solid State Commun.* **51** 951 (1984).

²¹H. Itoh, K. Murakami, K. Takita, and K. Masuda, in *Proceedings of the 14th International Conference on Defects in Semiconductors*, edited by H. J. von Bardeleben (Materials Science Forum, 1986), Vols. 10-12, p. 899.

²²G. G. Deleo, W. B. Fowler, and G. D. Watkins, *Phys. Rev. B* **29** 3193 (1984).

²³R. P. Messmer and P. A. Schultz, *Solid State Commun.* **52**, 563 (1984).

²⁴H. P. Hjalmarson and D. R. Jennison, *Phys. Rev. B* **31**, 1208 (1985).

²⁵F. Shimura and R. S. Hockett, *Appl. Phys. Lett.* **48**, 224 (1986).

²⁶H. J. Stein, in *Proceedings of Materials Research Symposium on Microscopic Identification of Electronic Defects in Semiconductors*, edited by N. M. Johnson, S. G. Bishop, and G. D. Watkins (Materials Research Society, Pittsburgh, 1985), p. 287.

²⁷D. K. Brice, in *Ion Implantation Range and Energy Deposition Distributions* (Plenum, New York, 1975).

²⁸K. Murakami, K. Masuda, K. Gamo, and S. Namba, *Appl. Phys. Lett.* **30**, 300 (1977).

²⁹M. Tamura, N. Natsuaki, and T. Tokuyama, in *Laser and Electron Beam*

Processing of Materials, edited by C. W. White and P. S. Peercy (Academic, New York, 1980), p. 247.

³⁰A. G. Cullis, H. C. Webber, J. M. Poate, and N. G. Chew, *J. Microsc.* **118**, 41 (1980).

³¹Y. Mada and N. Inoue, *Appl. Phys. Lett.* **48**, 1205, (1986).

³²See, for example, G. S. Oehrlein and J. W. Corbett, in *Proceedings of Materials Research Society Symposium on Defects in Semiconductors II*, edited by S. Mahajan and J. W. Corbett (Elsevier, New York, 1983), p. 107.

³³S. T. Pantelides and C. T. Sah, *Phys. Rev. B* **10**, 638 (1974).

³⁴K. L. Wang, *J. Appl. Phys.* **53**, 449 (1982).